J Wood Sci (2010) 56:118–126
DOI 10.1007/s10086-009-1078-5

ORIGINAL ARTICLE

Kiho Jung · Akihisa Kitamori · Kohei Komatsu

Development of a joint system using a compressed wooden fastener II: evaluation of rotation performance for a column-beam joint

Received: January 14, 2009 / Accepted: July 28, 2009 / Published online: December 16, 2009

Abstract In the present study, a plate and a doweled fastener made of compressed wood (CW) were newly introduced into a moment resisting column-beam joint system for a small portal frame structure. A mechanical model that contains not only an axial spring, but also a rotational spring, considered resistant factors to verify how each element resists rotation. Theoretical performance was compared with experimental data. Consequently, the mechanical model was shown to be suitable and the combination of resisting factors was found to be very effective; i.e., the rotational spring provides more influence on the stiffness and moment compared with the axial spring. Large moment and ductility can be achieved by virtue of the high embedding performance of the CW plate in the rotational spring, accompanied with the high shearing performance of the CW dowel in the axial spring.

Key words Moment resisting joint · Semirigid portal frame · Axial spring · Rotational spring

Introduction

The importance of the semirigid portal frame is increasing with the demand for more spacious accommodations in Japanese residential houses constructed of wood. The moment resisting joint system is important because the moment resisting joint is the only moment resisting factor. Many kinds of steel fasteners have been used in the moment resisting joint system because of high strength and reliability.

Now, many trials on portal frame structures are being conducted, aiming to reduce the use of steel fasteners with keeping a high moment carrying capacity, because steel may have several disadvantages such relatively high energy consumption in production, heterogeneity, disharmony with timber, rust problems, and so on when used in conjunction with timber structures. These considerations have energized research into the development of new joint systems composed with fasteners using environmentally friendly natural composite materials.[1]

With this trend, compressed wood (CW) was introduced as a fastener in a joint system.[2–4] Compressed wood may be suitable for use as a fastener in locations where severe stress concentration occurs, by virtue of its advantageous material properties and high density. The potential of a newly designed column-sill joint system using a CW fastener was verified, and the rotational spring effect by a CW plate is much higher than the dowel effect, as shown in a previous report.[5]

In the present research, a new column-beam joint design based on previous results[3,5] was suggested, as a moment resisting joint system for a semirigid portal frame system. Specifically, a mechanical model was developed and compared with experimental results to optimize the design. The ultimate goal of the present project is the development of a metal-free, eco-friendly timber joint system for use in Japanese residences.

Theory

The design of a column-beam joint using a compressed wooden plate and a dowel is shown in Fig. 1. The basic concept for good performance of a CW plate and a dowel is similar to that of the column-sill joint.[5]

As the rotational resisting factor for the joint, two CW plates (total, four plates) are located on the upper and lower border areas of the beam because high rotational performance could be expected,[5] and dowels are driven into the center of each CW plate to fix the CW plate to the column

K. Jung (✉) · A. Kitamori · K. Komatsu
Research Institute for Sustainable Humanosphere, Kyoto University, Gokasyou, Uji, Kyoto 611-0011, Japan
Tel. +81-774-38-3670; Fax +81-774-38-3678
e-mail: jungkiho@rish.kyoto-u.ac.jp

Part of this report was presented at the 59th Annual Meeting of Japan Wood Research Society in Matsumoto, March 2009

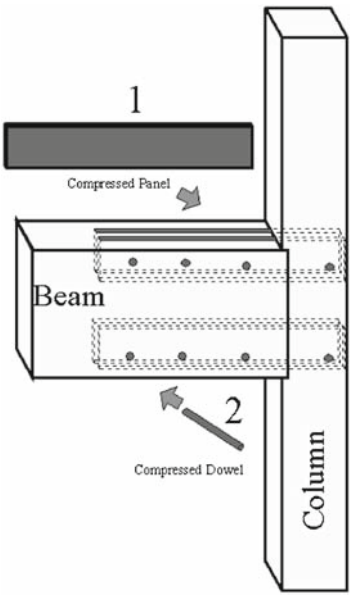

Fig. 1. Column-beam joint

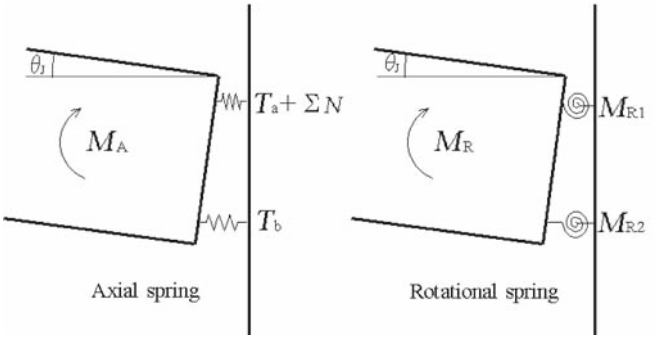

Fig. 2. Two types of springs

and beam. Two rotational areas by CW plates are more effective than that of one area because the rotational spring effect by a CW plate is much higher than the dowel effect.

This type of joint method can be expected to have two resisting factors against the rotational moment of the entire joint (Fig. 2). In the first type, two differently positioned CW plates act as axial springs through the shearing resistance of the dowel for tension and compression caused by joint rotation. In the second type, the rotational springs generated by the contact stress between each joint member satisfy the equilibrium of force perpendicular to the CW plate axis at each part of the joint. Because the embedding performance of CW is much higher than that of normal wood, by virtue of the exponential increase in the material property in accordance with the compression ratio, this is a type of effect by embedding resistance[11,12] and can be expected to have a high influence on the rotational behavior of the joint.

Balanced with the shearing and embedding performance of the dowel between the CW plate and the base member in these two resistance factors, this joint can be expected to achieve not only high strength but also high ductility by appropriate design. The relationship between the two types of springs for the rotational moment of the entire joint can be expressed as the total of two different moment components by the following equation:

$$M_{\text{Joint}} = M_{\text{A}} + M_{\text{R}} = (R_{\text{A}} + R_{\text{R}})\theta_{\text{J}} \tag{1-1}$$

where M_{A} is the moment derived from the axial spring, M_{R} is the moment derived from the rotational spring, and θ_{J} is the rotational angle of the entire joint.

Stiffness

Moment derived from axial spring

The mechanism of the moment–rotation relationship from axial springs is similar to the semirigid column-beam joint drawn with tension bolts.[6] Since the CW plate is fixed by a CW dowel at each area, the factors resisting axial force in the longitudinal direction are the tensile resisting factor (T_{a}) of the CW plate on the tensile area, the compressive resisting factor (T_{b}) of the CW plate, and the embedding resisting factor (ΣN) between the column and the beam on the compression area.

If λ is assumed to be the distance from the edge of the beam to the rotational center of the compression area, the equilibrium of force can be expressed by the following equation:

$$T_{\text{a}} + \sum N = T_{\text{b}} \tag{1-2}$$

The tensile and compressive stiffness (K_{T}) of the CW plate between the column and the beam is thought to be the combination of axial springs arranged in series derived from the shearing resistance of the CW dowel on two areas, assuming that there is no tensile or bending deformation on the CW plate.

$$K_{\text{T}} = \frac{K_{\text{d(Column)}} \cdot K_{\text{d(Beam)}}}{K_{\text{d(Column)}} + K_{\text{d(Beam)}}}, \quad K_{\text{d(Beam)}} = n_{\text{C}} n_{\text{P}} K_{\text{b0p0d0}}, \quad K_{\text{d(Column)}} = n_{\text{S}} n_{\text{P}} K_{\text{b90p0d0}} \tag{1-3}$$

The deformation (δ_{T}) by the tensile force of the CW plate for base-members can be obtained by the following equation:

$$\delta_{\text{T}} = \frac{T_{\text{b}}}{K_{\text{T}}} \tag{1-4}$$

Based on the geometric relationship between upper and lower CW plates, the following equation is obtained:

$$\delta_{\text{T}} = \left(l - \lambda - \frac{W}{2}\right)\theta_{\text{J}} \tag{1-5}$$

Equations 1-2 through 1-5 can be used to express the resisting forces for each resisting factor as follows:

$$T_{\text{a}} = K_{\text{T}}\left(\lambda - \frac{W}{2}\right)\theta_{\text{J}}, \quad T_{\text{b}} = K_{\text{T}}\left(l - \lambda - \frac{W}{2}\right)\theta_{\text{J}}, \quad \sum N = \frac{\lambda^2 (T - n_{\text{P}} t) C_{\text{y}} E_{90}}{2Z_0}\left\{1 + \frac{4Z_0}{3\lambda}\left(1 - e^{\frac{3x_1}{2Z_0}}\right)\right\}\theta_{\text{J}} \tag{1-6}$$

Substituting Eq. 1-6 into Eq. 1-2 yields the following equation:

$$T_b - T_a = \frac{\lambda^2 (T - n_P t) C_y E_{90}}{2Z_0} \left\{ 1 + \frac{4Z_0}{3\lambda} \left(1 - e^{\frac{3x_1}{2Z_0}} \right) \right\} \theta_J \tag{1-7}$$

and the length to the rotational center (λ) can be calculated as follows:

$$\lambda = \sqrt{\frac{2\beta l}{\alpha} + \left(\frac{(4\beta + \alpha\gamma)}{2\alpha} \right)^2} - \frac{(4\beta + \alpha\gamma)}{2\alpha}$$
$$\alpha_3 = (T - n_P t) C_y E_{90}, \quad \beta_3 = K_T Z_0, \quad \gamma_3 = \left\{ \frac{4Z_0}{3} \left(1 - e^{\frac{3x_1}{2Z_0}} \right) \right\} \tag{1-8}$$

Thus, moment (M_A) and stiffness (R_A) derived from the axial springs can be calculated by substituting the input factors mentioned in the above equations into the following equations:

$$M_A = T_a \left(\lambda - \frac{W}{2} \right) + T_b \left(l - \lambda - \frac{W}{2} \right) + \sum N \tag{1-9}$$

$$R_A = K_T \left(\lambda - \frac{W}{2} \right)^2 + K_T \left(l - \lambda - \frac{W}{2} \right)^2 + \frac{\lambda^2 (T - n_P t) C_y E_{90}}{2Z_0} \left\{ 1 + \frac{4Z_0}{3\lambda} \left(1 - e^{\frac{3x_1}{2Z_0}} \right) \right\} \tag{1-10}$$

Moment derived from the rotational spring

Each CW plate works independently as a rotational spring at each position by the cooperative work of the shearing resistance of the dowel and the embedding resistances of the CW plate.

This mechanism of force delivery is similar to that reported in a previous paper.[5] However, the resisting factor of contact between the CW plate and the beam must be added in this case.

First, the rational moment at each position is given by the following equation by considering the slope of the moment on the beam:

$$M_R = M_{R1} + M_{R2}, \quad M_{R1} = \left(\frac{H}{H - h} \right) M_{bh1} = M_{ch1},$$
$$M_{R2} = \left(\frac{H}{H - h} \right) M_{bh2} = M_{ch2} \tag{2-1}$$

where M_{R1} and M_{R1} are moments of CW plate-1 and CW plate-2 derived from the rotational spring on the entire joint area, M_{bh1} and M_{bh2} are moments of CW plate-1 and CW plate-2 derived from the rotational spring on the beam area, and M_{ch1} and M_{ch2} are moments of CW plate-1 and CW plate-2 derived from the rotational spring on the column area. Here, it was assumed that there is no bending or shearing deformation on the CW plate.

Stress and deformation angle are correlated as follows:

$$\theta_J = \theta_{b1} + \theta_{c1} = \theta_{b2} + \theta_{c2}, \quad R_{R1}\theta_J = R_{ch1}\theta_{c1} = \left(\frac{H}{H - h} \right) R_{bh1}\theta_{b1},$$
$$R_{R2}\theta_J = R_{ch2}\theta_{c2} = \left(\frac{H}{H - h} \right) R_{bh2}\theta_{b2} \tag{2-2}$$

where θ_{b1} and θ_{b2} are the rotational angles of CW plate-1 and CW plate-2, respectively, on the beam area, and θ_{c1} and θ_{c2} are the rotational angles of CW plate-1 and CW plate-2, respectively, on the column area.

Beam area

Resisting factors by CW plate-1 against the rotational moment on the beam area are the shearing resistance of the dowel and the embedding resistance between the CW plate and the beam, which can be expressed as follows[8,9]:

$$Q_{b1} = A_1 |X_{P1} - h_{be}| \theta_{b1}, \quad Q_{b2} = A_1 \left(h_{be} + \frac{h_{bd}}{2} - X_{P1} \right) \theta_{b1},$$
$$Q_{b3} = A_1 (h_{be} + h_{bd} - X_{P1}) \theta_{b1}, \quad C_{b1} = \frac{1}{2} A_2 X_{P1}^2 \theta_{b1},$$
$$C_{b2} = \frac{2}{3} A_2 (l - W) X_{P1} \theta_{b1} \tag{2-3}$$
$$A_1 = n_P K_{b90p90d90}, \quad A_2 = \frac{n_P t E_{(Beam90)}}{(l - W)}$$

where n_p is the number of CW plate at each area, $K_{b90p90d90}$ is stiffness of dowel for each direction, and $E_{(Beam90)}$ is embedding stiffness at beam area.

Here, the tangential Young's modulus of CW with a compressed ratio of 62% is five times higher than that of normal Japanese cedar.[7] Moreover, the height of the CW plate is one-third that of the beam. Thus, the embedding deformation of the CW plate can be ignored.

To determine the direction of Q_{b1}, two situations are considered as $X_{p1} \geq$ is larger or smaller than h_{be} ($X_{p1} \geq h_{be}$ or $X_{p1} \leq h_{be}$).

The equilibrium of the stress and the moment for CW plate-1 on the beam area yields the following equations:

$$P + Q_{b1} + C_{b1} + C_{b2} = Q_{b2} + Q_{b3},$$
$$PH + \left(h_{bp} - \frac{1}{3} X_{P1} + \frac{Z_0}{2} \right) C_{b1} + \left(h_{bp} + \frac{Z_0}{2} \right) C_{b2} + (\alpha_1 + h_{bd}) Q_{b1} - \left(\alpha_1 + \frac{h_{bd}}{2} \right) Q_{b2} - \alpha_1 Q_{b3} = 0 \ (X_{P1} \geq h_{be}) \tag{2-4}$$

$$P + C_{b1} + C_{b2} = Q_{b1} + Q_{b2} + Q_{b3},$$
$$PH + \left(h_{bp} - \frac{1}{3} X_{P1} + \frac{Z_0}{2} \right) C_{b1} + \left(h_{bp} + \frac{Z_0}{2} \right) C_{b2} - (\alpha_1 + h_{bd}) Q_{b1} - \left(\alpha_1 + \frac{h_{bd}}{2} \right) Q_{b2} - \alpha_1 Q_{b3} = 0 \ (X_{P1} \leq h_{be}) \tag{2-5}$$
$$\alpha_1 = h_{be} + \frac{Z_0}{2}, \quad h_{bp} = 2h_{be} + h_{cd}$$

By substituting the former equation into the latter equation in Eqs. 2-4 and 2-5, the following cubic equation can be obtained:

$$X_{P1}^3 + \frac{3(2H - 2h_{bp} - Z_0)}{2} X_{P1}^2 + 9A_1 (2H - 2\alpha_1 - h_{bd}) + 2A_2 l (2H - 2h_{bp} - Z_0) + \frac{2A_2 W (2h_{bp} - 2H + Z_0)}{A_2} X_{P1} + \frac{18A_1 h_{be} (2\alpha_1 - 2H + h_{bd}) + 3A_1 h_{bd} (6\alpha_1 - 6H + h_{bd})}{2A_2} = 0 \tag{2-6}$$

By substituting cubic Eq. 2-6 into the following equation, the distance to the rotational center (X_{p1}') can be calculated:

$$X_{P1} = \sqrt[3]{-\left(\frac{27c+2a^3-9ab}{54}\right)+\sqrt{\left(\frac{27c+2a^3-9ab}{54}\right)^2+\left(\frac{3b-a^2}{9}\right)^3}}+\sqrt[3]{\left(\frac{27c+2a^3-9ab}{54}\right)-\sqrt{\left(\frac{27c+2a^3-9ab}{54}\right)^2+\left(\frac{3b-a^2}{9}\right)^3}}-\frac{1}{3}a \quad (2\text{-}7)$$

$$a = \frac{3(2H-2h_{bp}-Z_0)}{2},$$

$$b = \frac{9A_1(2H-2\alpha_1-h_{bd})+2A_2l(2H-2h_{bp}-Z_0)+2A_2W(2h_{bp}-2H+Z_0)}{A_2},$$

$$c = \frac{18A_1h_{be}(2\alpha_1-2H+h_{bd})+3A_1h_{bd}(6\alpha_1-6H+h_{bd})}{2A_2}$$

Thus, stiffness (R_{bh1}) for plate-1 can be expressed by the following equation:

$$R_{bh1} = A_1(X_{P1}-h_{be})^2 + A_1\left(h_{be}+\frac{h_{bd}}{2}-X_{P1}\right)^2 + A_1(h_{be}+h_{bd}-X_{P1})^2 + \frac{1}{3}A_2{X_{P1}}^3 + \frac{2}{3}A_2(l-W){X_{P1}}^2 + \frac{1}{2}\left(\frac{1}{2}A_2{X_{P1}}^2+\frac{2}{3}A_2(l-W)X_{P1}\right)\mu W \quad (2\text{-}8)$$

The resisting mechanism of CW plate-2 for the rotational moment is slightly different from that of CW plate-1. CW plate-2 reacted in full compression for the beam area, whereas CW plate-2 reacts in partial compression for the beam area. These two different positions of the CW plates are reversed upon embedding for the rotational direction. To determine the direction of Q_{b1}, the two situations considered for plate-1 are also considered for plate-2.

$$Q'_{b1} = A'_1(X_{P2}-h_{be})\theta_{b2}, \quad Q'_{b2} = A'_1\left(X_{P2}-h_{be}-\frac{h_{bd}}{2}\right)\theta_{b2},$$
$$Q'_{b3} = A'_1|(h_{bd}+h_{be})-X_{P2}|\theta_{b2},$$
$$C'_{b1} = \frac{1}{2}A'_2(h_{bp}-X_{P2})^2\theta_{b2}$$
$$A'_1 = n_P K_{b90p90d90}, \quad A'_2 = \frac{n_P t E_{(Plate90+Beam90)}}{(l-W)} \quad (2\text{-}9)$$

where n_p is the number of CW plates for each area, $K_{b90p90d90}$ is stiffness of the dowel for each direction, and $E_{(Plate90+Beam90)}$ is the embedding stiffness for the beam area.

The equilibrium of the stress and the moment for CW plate-2 on the beam area yield the following equations:

$$P+Q'_{b1}+Q'_{b2} = Q'_{b1}+C'_{b1},$$
$$PH+(\alpha'_1+h_{bd})Q'_{b1}+\left(\alpha'_1+\frac{h_{bd}}{2}\right)Q'_{b2}-\alpha'_1Q'_{b3}-\left(\frac{1}{3}h_{bp}+\frac{2}{3}X_{P2}+\frac{Z_0}{2}\right)C'_1 = 0\ (X_{P2}\le h_{be}+h_{bd}) \quad (2\text{-}10)$$

$$P+Q'_{b1}+Q'_{b2}+Q'_{b3} = C'_{b1},$$
$$PH+(\alpha'_1+h_{bd})Q'_{b1}+\left(\alpha'_1+\frac{h_{bd}}{2}\right)Q'_{b2}+\alpha'_1Q'_{b3}-\left(\frac{1}{3}h_{bp}+\frac{2}{3}X_{P2}+\frac{Z_0}{2}\right)C'_1 = 0\ (X_{P2}\ge h_{be}+h_{bd}) \quad (2\text{-}11)$$
$$\alpha'_1 = h_{be}+\frac{Z_0}{2}, \quad h_{bp} = 2h_{be}+h_{cd}$$

Substituting the former into the latter equation, the following cubic equation can be obtained:

$$X_{P2}^3 + \frac{3(Z_0-2h_{bp}-2H)}{4}X_{P2}^2 + \frac{9A'_1(2H-2\alpha'_1-h_{bd})+3A'_2h_{bp}(2H-Z_0)}{2A'_2}X_{P2} + \frac{18A'_1h_{be}(2\alpha'_1-2H+h_{bd})+3A'_1h_{bd}(6\alpha'_1+h_{bd}-6H)+A'_2h_{bp}^2(2h_{bp}-6H+3Z_0)}{4A'_2} = 0 \quad (2\text{-}12)$$

By solving cubic Eq. 2-12 for X_{p2} in the same way as for CW plate-1, the distance to the rotational center (X_{p2}) can be calculated with the factors shown in the following equation:

$$a = \frac{3(Z_0-2h_{bp}-2H)}{4},$$

$$b = \frac{9A'_1(2H-2\alpha'_1-h_{bd})+3A'_2h_{bp}(2H-Z_0)}{2A'_2},$$

$$c = \frac{18A'_1h_{be}(2\alpha'_1-2H+h_{bd})+3A'_1h_{bd}(6\alpha'_1+h_{bd}-6H)+A'_2h_{bp}{}^2(2h_{bp}-6H+3Z_0)}{4A'_2} \quad (2\text{-}13)$$

Thus, the stiffness (R_{bh2}) of plate-2 can be calculated as follows:

$$R_{bh2} = A'_1(X_{P2}-h_{be})^2 + A'_1\left(X_{P2}-h_{be}-\frac{h_{bd}}{2}\right)^2 + A'_1(h_{bd}+h_{be}-X_{P2})^2 + \frac{1}{3}A'_2(h_{bp}-X_{P2})^3 + \frac{1}{2}\left(\frac{1}{2}A'_2(h_{bp}-X_{P2})^2\right)\mu W \quad (2\text{-}14)$$

Column area

First, it was assumed that two differently positioned CW plates at the joint have the same rotational moment on the column area. The rotational stiffness by the shearing resistance of the dowel and the embedding resistance of the CW plate on the column area can be calculated by modifying the mechanical model proposed in part 1 of this research.[5]

Each rotational center (X_P) of two differently positioned CW plates on the column area can be calculated by the following equation:

$$X_P = \frac{3B_1\beta_1(Z_0 - h_{cd} - 2\beta_3) + 3B_1\beta_2(Z_0 + h_{cd} - 2\beta_3) + B_2Z_0^2(Z_0 - 3\beta_3)}{6B_1(Z_0 - 2\beta_3) + 4B_2W(Z_0 - \beta_3) + 3B_2Z_0(Z_0 - 2\beta_3)}$$
$$B_1 = n_P \cdot K_{b0p90d90}, \quad B_2 = n_P \cdot t \cdot K_{(Plate90+Column0)}, \quad \beta_1 = \frac{Z_0 + h_{sd}}{2},$$
$$\beta_2 = \frac{Z_0 - h_{sd}}{2}, \quad \beta_3 = Z_0 + h_{ce} + h_{cd} - X'_P \tag{3-1}$$

The combination ($E_{(plate90+Column0)}$) of the embedding stiffness of the CW plate and the column can be calculated b y the following equation:[7]

$$K_{(Plate90+Column0)} = \frac{K_{(Plate90)} \cdot K_{(Column0)}}{K_{(Plate90)} + K_{(Column0)}} \tag{3-2}$$
$$K_{(Plate90)} = \frac{E_{(CW90)}}{Z_0} K_{(Cedar0)} = \frac{E_{(Cedar0)}}{31.6 + 10.9 \cdot t}$$

Each stiffness (R_{ch1}, R_{ch2}) of the two differently positioned CW plates on the column area can be calculated by the following equation:

$$R_{ch1} = B_1(\beta_1 - X_P)^2 + B_1(X_P - \beta_2)^2 + \frac{1}{3}B_2(Z_0 - X_P)^3 + \frac{1}{3}B_2X_P^3 + \frac{2}{3}B_2WX_P^2 + \frac{1}{2}\left(\frac{1}{2}B_2(Z_0 - X_P)^2 + \frac{1}{2}B_2X_P^2 + \frac{2}{3}B_2WX_P\right)\mu W \tag{3-3}$$

where μ (= 0.35) is the coefficient of friction between the CW plate and the column.[11]

Yielding moment

Yielding of the entire joint is thought to be determined by the yielding of each of the two different types of parallel springs. The yielding moment ($M_{y\text{-}A}$) derived from the axial spring will be decided by the yielding caused by the shearing of the dowel at the CW plate of the tensile area. In addition, the yielding moment ($M_{y\text{-}R}$) derived from the rotational spring will be decided by the yielding of the shearing and embedding of the dowel between the beam and the CW plate and between the CW plate and the column. The two yielding points (M_{y1}, M_{y2}) of the joint were determined by summing the two yielding points ($M_{y\text{-}A}$, $M_{y\text{-}R}$) of the spring. Here, to avoid doubling the yielding moment of the CW dowel, only the yielding for the axial spring was considered. Hence, only yielding by embedding was considered for the moment derived from the rotational spring.

Yielding moment derived from the axial spring

The yielding strength ($P_{y\text{-}A}$) of dowel shearing at two areas due to axial force can be calculated by the following equation:

$$P_{y-A} = \min\left(P_{y(Beam)}, P_{y(Column)}\right) \tag{4-1}$$
$$P_{y(Beam)} = n_B P_{y(b0p0d0)}, \quad P_{y(Column)} = n_C P_{y(b90p0d0)}$$

where $P_{y(b0p0d0)}$ and $P_{y(b90p0d0)}$ are the yielding strengths of dowel for each direction.

When the tensile force (T_b) for the CW plate reaches the yielding point of the shearing of the dowel, the joint is assumed to yield. At this time, the yielding angle ($\theta_{y\text{-}A}$) and moment ($M_{y\text{-}A}$) derived from the axial spring can be calculated by the following equation:

$$M_{y-A} = R_A \cdot \theta_{y-A}, \quad \theta_{y-A} = \frac{P_{y-A}}{K_T\left(l - \lambda - \frac{W}{2}\right)} \tag{4-2}$$

Yielding moment derived from the rotational spring

In the determination of the yielding moment ($M_{y\text{-}R}$) derived from the rotational spring, yielding by the shearing of the dowel as a result of the force perpendicular to the plate axis direction on each area and embedding at the column area were considered. The lowest value of the moment calculated in this manner is defined as the yielding moment derived from the rotational spring as follows:

$$M_{y-R} = \min\left[M_{y-d(Beam)}, M_{y-d(Column)}, M_{y-CW}, M_{y-Column}\right] \tag{4-3}$$

Beam area

When the shearing force of the dowel at the most distant point from each rotational center (X_{P1}, X_{P2}) reaches the yielding strength ($P_{y\text{-}d(Beam)}$) of the dowel on the beam area, the yielding angle ($\theta_{b1y\text{-}d(Beam)}$, $\theta_{b2y\text{-}d(Beam)}$) for each differently positioned plate can be calculated by the following equation:

$$\theta_{b1y-d(Beam)} = \left\{\frac{P_{y-d(Beam)}}{A_1(h_{be} + h_{bd} - X_{P1})}\right\},$$
$$\theta_{b2y-d(Beam)} = \left\{\frac{P_{y-d(Beam)}}{A'_1(X_{P2} - h_{be})}\right\} \tag{4-4}$$
$$P_{y-d(Beam)} = n_P P_{y(b90p90d90)}, \quad A_1 = n_P K_{b90p90d90},$$
$$A'_1 = n_P K_{b90p90d90}$$

Here, it is assumed that no splitting occurs in the base member of the CW plate.

Thus, the yielding moment ($M_{y\text{-}d(Beam)}$) on the beam area can be calculated using lower value between differently positioned CW plates, while considering the moment arm and the rotational angle between the beam and the column, as shown in the following equation:

$$M_{y-d(Beam)} = \min\left\{R_{bh1} \cdot \theta_{b1y-d(Beam)}\left(1 + \frac{1}{R_{bh2}}\right), R_{bh1} \cdot \theta_{b2y-d(Beam)}\left(1 + \frac{1}{R_{bh1}}\right)\right\} \cdot \left(\frac{H}{H - h}\right) \tag{4-5}$$

Column area

The determination of the yielding moment on the column area is performed by a procedure similar to that for the

case of the beam, but there is no difference in resistance among differently placed CW plates. The yielding moment ($M_{\text{y-d(Column)}}$) for each plate on the column area can be calculated by the following equation:

$$M_{\text{y-d(Column)}} = R_{\text{S}} \cdot \theta_{\text{y-d(Column)}}, \quad \theta_{\text{y-d(Column)}} = \left\{ \frac{P_{\text{y-d(Column)}}}{B_1(\beta_1 - X_{\text{P}})} \right\}$$
$$P_{\text{y-d(Column)}} = n_{\text{P}} P_{\text{y(b0p90d90)}}, \quad B_1 = n_{\text{P}} K_{\text{b0p90d90}} \tag{4-6}$$

The yielding moment ($M_{\text{y-CW}}$) generated by embedding the CW plate in the column can be calculated according to Inayama's theory[8]:

$$M_{\text{y-CW}} = R_{\text{R}} \cdot \theta_{\text{y}}, \quad \theta_{\text{y-CW}} = \frac{WF_{\text{m}}}{X_{\text{P}} E_{\perp} \sqrt{C_{\text{x}} C_{\text{xm}} C_{\text{ym}}}},$$
$$C_{\text{x}} = 1 + \frac{2W}{3X_{\text{P}}}\left(2 - e^{-\frac{3x_1}{2W}}\right), \quad C_{\text{xm}} = 1 + \frac{4W}{3X_{\text{P}}}, \quad C_{\text{ym}} = 1 + \frac{4W}{3nn_{\text{P}}t} \tag{4-7}$$

The yielding moment ($M_{\text{y-Column}}$) generated by the embedding of the column can be calculated by the following equations (Eq. 4-8)[5]:

$$M_{\text{y-Column}} = R_{\text{R}} \cdot \theta_{\text{y-Column}}, \quad \theta_{\text{y-Column}} = \frac{n_{\text{P}} t X_{\text{P}} F_{\text{C}} \theta_{\text{S}}}{2(N_2 + N_3)} \tag{4-8}$$

where $F_{\text{c}} = 60.68\ \rho$ and ρ is density of wood. The compressive stress is assumed to have a triangular distribution.

Experimental methods

CW plates of 420 mm × 80 mm × 15 mm and dowels of diameter 12 mm (Ø) having different parameters were used. The construction method and material properties of CW fasteners were the same as those was described in a previous report.[5] Four plates and six, eight, and ten dowels, respectively, were used on each parameter, and three specimens were prepared for each.

Each parameter was determined by the number of dowels, as shown in Table 1 and Fig. 6.

For the base member, two types of Japanese cedar glulams, which grade is 6 GPa in Young's modulus, 225 MPa in modulus of rupture (MOR) were used for the column (120 mm × 120 mm × 1200 mm) and the beam (120 mm × 240 mm × 700 mm), respectively.

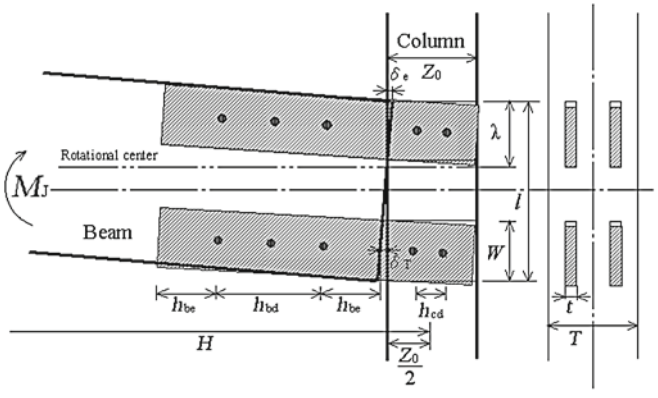

Fig. 3. Single column-beam joint for rotational moment

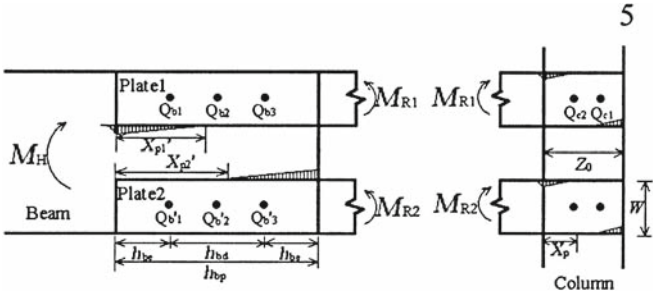

Fig. 4. Mechanical stress algorithm of two areas for the moment derived from the rotational spring (*left*, beam area; *right*, column area)

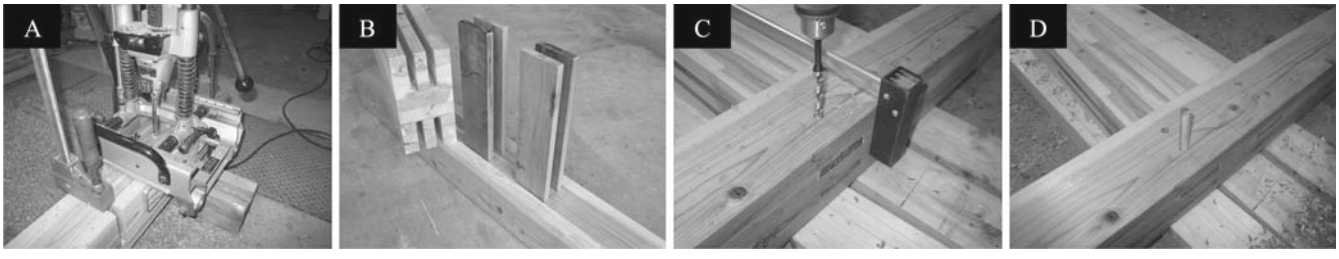

Fig. 5. Making and assembling process for column-beam joint: cutting (**A**), assembling (**B**); making hole (**C**); inserting dowel (**D**)

Table 1. Parameters for the column-beam joint for the rotational test

Specimen	Dimension				Number of dowels	
	Column (mm)	Beam (mm)	Panel (mm)	Dowel (φ)	Column	Beam
RCP4B4C2	120 × 120 × 1200	120 × 240 × 575	80 × 580 × 15	12	4	2
RCP4B6C2				12	6	2
RCP4B6C4				12	6	4

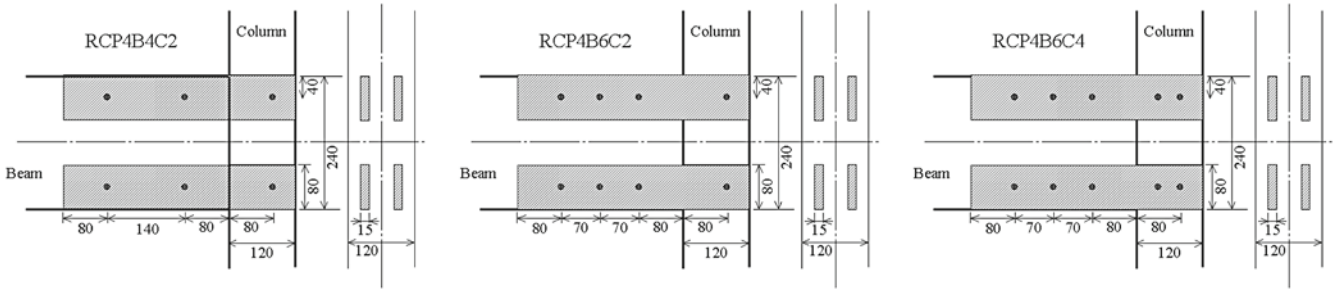

Fig. 6. Joint parameters

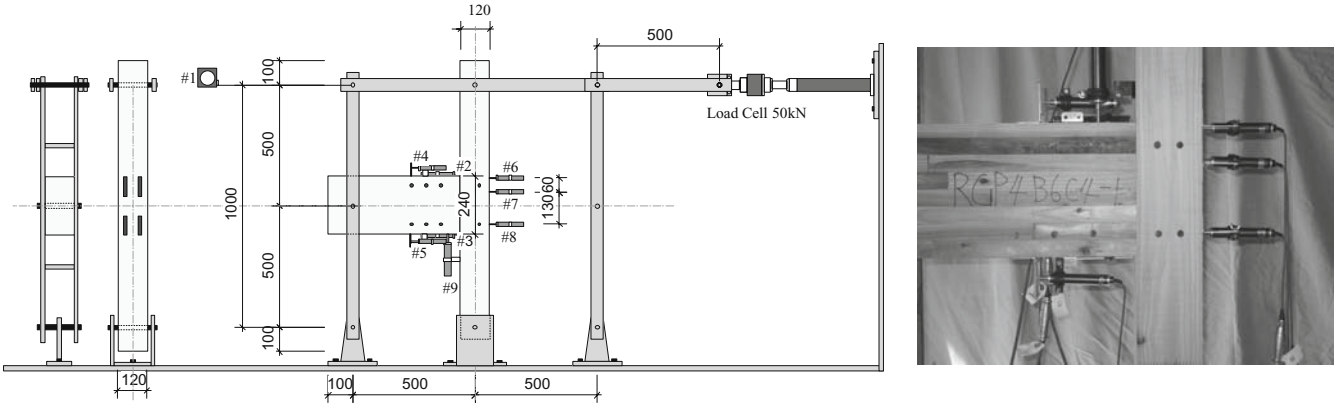

Fig. 7. Apparatus for the rotation test of the column-beam joint

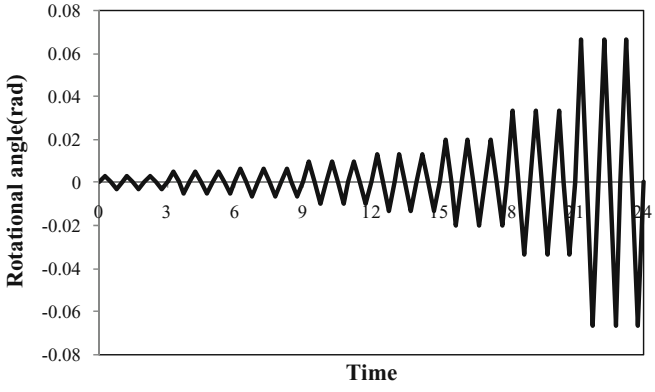

Fig. 8. Loading schedule

The construction and assembly process of the joint is shown in Fig. 5. A groove and a square hole were cut in the base members in advance using a mortiser. The joint was then assembled by inserting the CW plate. Finally, round holes were made using a drill from outside the joint, and a compressed dowel was then driven into each hole.

Figure 7 shows the experimental apparatus of the rotation test for the column-beam joint. For evaluating the performance under the rotational moment (M), a quadratic-link steel frame, which is connected by a steel pin having a 1000-mm span, was used. Each specimen was set up on the frame and was jointed with a steel pin (Ø, 22 mm), as shown in Fig. 7.

The rotational deformation of the joint was applied by this steel frame, which was controlled by a hydraulic actuator. The loading schedule was determined through a step displacement with angles of the steel frame of 1/300, 1/200, 1/150, 1/100, 1/75, 1/50, 1/30, and 1/15 rotational angle (rad) (transducer, DTP-500S) as shown in Fig. 8. At each step, three loading cycles were applied. The relative displacements between the plate and each member were measured by displacement transducers (CDP-25 and CDP-50) for estimating accurate rotational angles with the corresponding applied load measured by a 50-kN load cell.

Results and discussion

Figure 9 shows the moment versus the rotational angle response curves for all types of joints. Table 3 lists experimental values obtained by a perfect bilinear approximation in comparison of those calculated by mechanical model with each factor shown in Table 2.

In Fig. 10, the stiffness (R_A, R_R) and the yielding moment ($M_{y\text{-}A}$, $M_{y\text{-}R}$) calculated by the mechanical model for each moment derived from the axial spring and the rotational spring are shown separately, and the total stiffness (R_A + R_R) and yielding moment (M_{y1}, M_{y2}) of the entire joint obtained by superposing two factors were compared with the experimental envelope curve averaged for three specimens. Satisfactory agreement was obtained in each case.

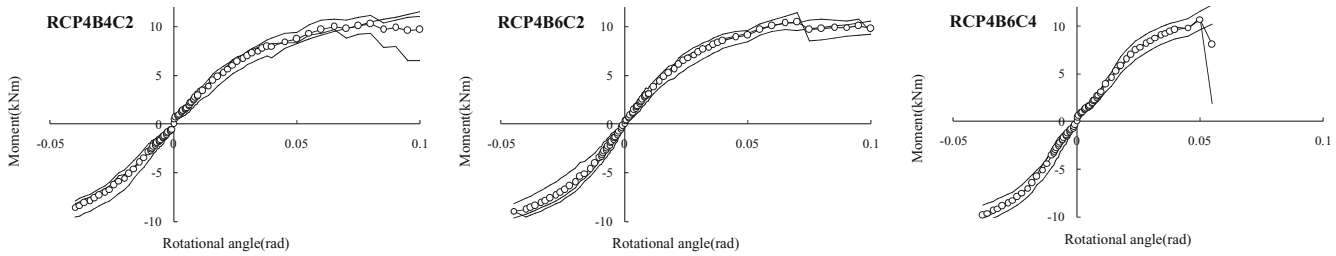

Fig. 9. Moment versus rotational angle (*rad*)

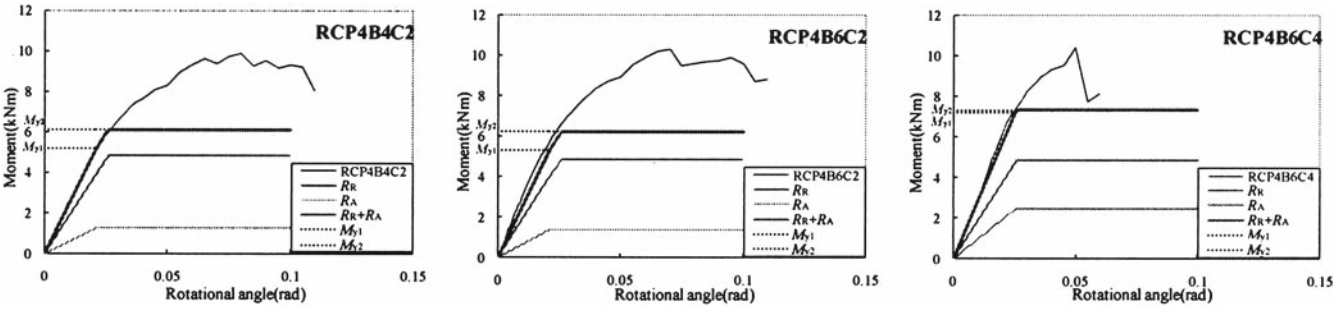

Fig. 10. Comparison of experimental and calculated values for each area column-beam joint

Table 2. Parameters for calculating by mechanical model

Double shear property of dowel								Compression property				Coefficient of friction	Density (g/cm^3)
Stiffness (N/mm)				Yielding strength (N)				Elastic modulus (N/mm^2)			Yielding (N/mm^2)		
K_{b0p0d0}	$K_{b90p90d90}$	$K_{b90p0d0}$	$K_{b0p90d90}$	$P_{yb0p0d0}$	$P_{yb90p90d90}$	$P_{yb90p0d0}$	$P_{yb0p90d90}$	$E_{(CW90)}$	$E_{(Cedar90)}$	$E_{(Cedar0)}$	$F_{m\text{-}CW}$	μ	ρ
3145	3519	2216	3470	5296	4166	4581	5619	1000	240	6000	45	0.35	0.33

Table 3. Comparison of calculated and experimental values

Specimen	Calculated values			Experimental values			
	R_{model}(kNm/rad)	$M_{y1\text{-}model}$(kNm)	$M_{y2\text{-}model}$(kNm)	R_{exp}(kNm/rad)	$M_{y\text{-}exp}$(kNm)	M_{max}(kNm)	E(Nmrad)
RCP4B4C2	246.8	5.2	6.1	258.9	5.9	10.0	432.4
RCP4B6C2	252.5	5.3	6.2	281.1	5.9	10.5	460.2
RCP4B6C4	284.2	7.2	7.3	313.7	7.3	11.9	471.5

R, Initial stiffness; M_y, yielding moment; M_{max}, maximum moment; E, energy

The stiffness of the rotational spring was 3.1, 2.9, and 1.9 times higher than that of the axial spring for the RCP4B4C2, RCP4B6C2, and RCP4B6C4 specimens, respectively; this is because the effect by embedding resistance[11,12] was effective due to the high compressive modulus of the CW plate.

The initial yielding was caused by the axial springs with the shearing of the dowel in the column area, and the subsequent yielding was caused by the rotational springs followed by the embedment yield of the CW plate at the column area.

The yielding moment ($M_{y\text{-}R}$) derived from the rotational spring is much higher than that ($M_{y\text{-}A}$) derived from the axial spring, which comprised 79%, 78%, and 66% of the yielding moment of the entire joint for the RCP4B4C2, RCP4B6C2, and RCP4B6C4 specimens, respectively. Thus, the axial spring was verified to give a supplemental effect for the yielding moment of whole joint. Large moment and ductility can be achieved in this process and provides a slight improvement in the moment carrying capacity. The performance of the entire joint, except for the RCP4B6C4 specimen, showed high ductility by virtue of the high deformational capacity of the CW dowel upon shearing.

Figure 11 shows each type of specimen at 1/10 rad. The RCP4B4C2 and RCP4B6C2 specimens are ductile until 0.1 rad. However, the RCP4B6C4 specimen failed relatively early in bending and split from the region at the column area in which the dowel was inserted. Therefore, it is thought

Fig. 11. Final stage of each type of joint on the rotational test

that a larger column is necessary to achieve better performance for the design of the RCP4B6C4 specimen.

Conclusion

In the present study, the rotational performance for the column-beam joint using CW fasteners was evaluated. The major conclusions of the present study are as follows:

1. To clarify the mechanism of this type of joint, a new mechanical model was developed that considers axial and rotational springs separately, and this was compared with experimental results.
2. The rotational behavior of the entire joint observed in an experiment was in good agreement with analytical estimates. Consequently, the mechanical model was found to be suitable.
3. The stiffness and moment derived from the rotational spring were dominant compared with those derived from the axial spring.
4. The moment carrying capacity of this joint is very effective because the rotational spring works in a manner similar to the effect by embedding resistance,[11,12] with high compressive mechanical properties of the CW plate, assisted by the shearing performance of the CW dowel, which acts as an axial spring.

Acknowledgments The present study was carried out with the support of the Japan Society for the Promotion of Science (JSPS).

References

1. Jung K, Kitamori A, Leijten AJM, Komatsu K (2006) Effect of changes in moisture content due to surrounding relative humidity on contact stress in traditional mortise and tennon joints. 3 (in Japanese). Mokuzai Gakkaishi 52:358–367
2. Nakata K, Komatsu K (2007) Development of timber portal frames compressed LVL plates and pins. 1 (in Japanese). Mokuzai Gakkaishi 53:313–319
3. Jung K, Kitamori A, Komatsu K (2008) Evaluation of structural performance of compressed wood as shear dowel. Holzforchung 62:461–467
4. Jung K, Kitamori A, Minami M, Komatsu K (2008): Development of joint system using compressed wooden fastener. CD. 10th World Conference on Timber Engineering, Miyazaki, Japan
5. Jung K, Kitamori A, Komatsu K (2008) Development of a joint system using a compressed wooden fastener. 1. J Wood Sci 55:273–282
6. Inayama M, Yamaguchi K, Miyada Y (2008) Study on structural design method of timber semi-rigid joints drawn with tensile blots. Summaries of technical papers of Annual Meeting Archirectural Institute of Japan. C-1, Structures III, pp 355–356
7. Kitamori A, Jung K, Mori T, Komatsu K (2010) Mechanical properties of compressed wood in accordance with compressed ratio (in Japanese). Mokuzai Gakkaishi (in press)
8. Allowable stress design method for timber housings (2007) Japan housing and Wood Technology Center, Tokyo, pp 56–58
9. Kitamori A, Jung K, Minami M, Komatsu K (2008) Evaluation on the stiffness of lattice shear wall. J Struct Eng 55B:109–116
10. Fukuyama H, Ando N, Inayama M, Takemura M, Inoue M (2007) Proposal of analytical models of wooden dowel shear joint. J Struct Constr Eng AIJ 622:129–136
11. Guan ZW, Kitamori A, Komatsu K (2007) Experimental study and FE modeling of Japanese "Nuki" joints, part one: initial stress states subjected to different wedge configurations. Eng Struct 30:2032–2040
12. Guan ZW, Kitamori A, Komatsu K (2007) Experimental study and FE modeling of Japanese "Nuki" joints, part two: racking resistance subjected to different wedge configurations. Eng Struct 30:2041–2049